Interpreting tracer breakthrough tailing in a conduit-dominated karstic aquifer

N. Massei · H. Q. Wang · M. S. Field · J. P. Dupont · M. Bakalowicz · J. Rodet

Abstract Breakthrough tailing has been observed during dye-tracing recovery tests in the Norville aquifer system (chalk), France. Karst-conduit flow and transport parameters were assessed using two different interpretative methods: the linear graphical method and the Chatwin method (implemented in the Qtracer2 program). The linear graphical method was used to model the observed tailing effects, which was explained by a second smaller delayed breakthrough curve. By comparing the results of tracer-test interpretation for the two methods, it was possible to relate the area of this second curve to the importance of turbulent flow in spring discharge. The more turbulent the flow, the less important the contribution of the second breakthrough curve and the tailing effect. The observed tailing could possibly be controlled by hydrodynamics to a greater extent than usually expected, the tailing effects being mostly attributed to diffusion phenomena. Tailing effects were expected to increase with discharge and the piezometric level, which would have resulted in overpressure in conduits, fissure flooding, etc. Instead, breakthrough tailing tended to disappear with increasing aquifer discharge, which would support the hypothesis of there being mostly hydrodynamic-controlled tailing effects instead of matrix- or fissure-diffusion.

Received: 26 September 2005 / Accepted: 29 October 2005
Published online: 26 January 2006

Disclaimer: The views expressed in this paper are solely those of the authors and do not necessarily reflect the views or policies of the U.S. Environmental Protection Agency. Mention of trade names or commercial products does not constitute endorsement or recommendation for use.

N. Massei (✉) · J. P. Dupont · J. Rodet
Département de Géologie, UMR CNRS 6143, Université de Rouen,
76821 Mont-Saint-Aignan Cedex, France
e-mail: nicolas.massei@univ-rouen.fr
Tel.: 33-(0)2-3514-6730
Fax: 33-(0)2-3514-7022

H. Q. Wang
Laboratoire de Mécanique, Physique et Géosciences, Université du Havre,
76058 Le Havre, France

M. S. Field
National Center for Environmental Assessment (8623D), Office of Research and Development, U.S. Environmental Protection Agency,
1200 Pennsylvania Ave., NW, Washington, DC 20460-0001, USA

M. Bakalowicz
CNRS, Hydrosciences, Université Montpellier II,
cc MSE,
34095 Montpellier, CEDEX 5, France

Résumé Des effets de traîne (ou ≪ effets de tailing ≫) ont été observés sur les courbes de restitution d'essais de traçage réalisés dans le système karstique de Norville (Haute-Normandie, France). Les propriétés de transport et hydrauliques ont été estimées au moyen de deux méthodes différentes d'interprétation : la Méthode Graphique Linéaire et la méthode de Chatwin (utilisée par le programme Qtracer2). La Méthode Graphique Linéaire a été utilisée pour modéliser les effets de traîne observés, qui ont été expliqués par une deuxième courbe de restitution retardée faisant partie de la courbe totale. En comparant les résultats des interprétations fournis par les deux méthodes, il s'est avéré possible de relier l'aire de cette seconde courbe à l'importance de l'écoulement turbulent dans le système : plus l'écoulement est turbulent, plus l'aire de cette deuxième courbe est petite et plus l'effet de traîne est faible. De tels effets, dans une grande majorité des cas expliqués par des phénomènes de double-porosité, peuvent donc être contrôlés par les conditions hydrodynamiques à un degré plus important que celui communément considéré. En effet, les effets de traîne observés auraient été supposés augmenter avec le débit et la charge dans le système, qui occasionneraient des phénomènes de surpression dans les conduits, de diffusion dans la fissuration, etc. En réalité, le fait que les effets de traîne tendent à disparaître quand le débit augmente soutiendrai l'hypothèse d'un contrôle hydrodynamique largement majoritaire dans leur génération, plutôt que d'attribuer de manière systématique cette génération des effets de traîne à des phénomènes de diffusion dans la porosité matricielle ou fissurale.

Resumen Se ha observado ruptura de colas durante pruebas de recuperación con trazadores de color en el sistema de acuífero carbonatado-arcilloso Norville, Francia. Se evaluaron flujo en conductos kársticos y parámetros de transporte utilizando dos métodos interpretativos distintos: el Método

 DOI 10.1007/s10040-005-0010-3

Gráfico Linear y el Método Chatwin (implementado en el programa Qtracer2). El Método Gráfico Linear se usó para modelizar los efectos observados de colas lo cual se explicó mediante una segunda curva de ruptura de retardo más pequeña. Mediante la comparación de los resultados de las pruebas de trazadores interpretadas de los dos métodos fue posible relacionar el área de esta segunda curva con la importancia de flujo turbulento en la descarga del manantial. Mientras más turbulento el flujo menos importante la contribución de la segunda curva de rompimiento y el efecto de cola. La cola observada podría ser controlada por la hidrodinámica en mayor medida a lo que normalmente se esperaría, con el efecto de cola la mayor parte del tiempo atribuido al fenómeno de difusión. Se esperaba que los efectos de cola incrementaran con la descarga y el nivel piezométrico lo cual daría por resultado sobrepresión en conductos, inundación en fracturas, etc. Sin embargo, la ruptura de cola tendió a desaparecer con la descarga creciente del acuífero lo cual apoyaría la hipótesis de efectos de cola con control hidrodinámico más que difusión en matriz o fisura.

Keywords Karst · Conduit flow · Tracer · Breakthrough tailing · Dispersivity

Introduction

According to Quinlan and Ewers (1985), "a tracer test is much more efficient than tens of bore holes for studying karst aquifers." In situ tracer experiments constitute one of the best means for characterizing the hydraulic and transport properties of karstic-flow systems. The quantitative analysis of tracer breakthrough curves can be useful for determining the structure/function relationships of karstic hydrosystems. Such studies constitute inverse approaches to the issue of mass transport within karstic aquifers. The most recent studies are helping to refine the quantitative analysis of transport properties associated with karstic aquifers. In most cases, these studies are based on the use of artificial tracers (Bracq et al. 1992; Cornaton and Perrochet 2002; Dzikowski et al. 1995; Field and Pinsky 2000; Grasso et al. 2003; Hauns et al. 2001; Maloszewski et al. 2002; Uliana et al. 2001; Wang and Crampon 1995; Wang et al. 1987; White 2002). Hauns et al. (2001) used laboratory experiments to assess the influence of various morphologies (channels, pools, rapids. . .) on the shape of the breakthrough curve. Other studies are more focused on the use of natural tracers such as isotopes, or major ionic species to delineate global flowpaths, very often at a more regional scale (Emblanch et al. 2003; Fairchild et al. 2000; Herczeg et al. 1997; Katz and Bullen 1996; Katz et al. 1998; Lee and Krothe 2001, 2003). On the other hand, more classical approaches have been used to identify the overall transport properties of karst systems by use of parameters such as electrical conductivity, turbidity, and particle size distribution (Desmarais and Rojstaczer 2002; Lacroix et al. 2000; Mahler and Lynch 1999; Massei et al. 2002). Other studies have considered these same aspects in a more quantitative way from a more mechanical point of view (Field 1997; Field and Pinsky 2000). Pinault et al. (2001) established transfer functions for the quick-flow, slow-flow, delayed infiltration components by linear systems-based analysis of major ionic species time series.

All these approaches have a common objective, which is the differentiation of the various functional compartments and reservoirs involved in hydrodynamic behaviour and mass transport. Artificial tracer tests are a relatively easy means of studying the transport properties of karstic aquifers. The purpose of this study is to compare two methods of breakthrough curve analysis for estimating dispersive parameters in a karst system in northwestern France.

Study site and methods

Geomorphological and geological settings

The Norman climate (northwestern coast of France) is typically oceanic. Average temperatures are approximately 10–12 °C and average annual precipitation ranges between 600 and 1,100 mm.

The topography of the Haute-Normandie region is characterized by moderate relief (<300 m). To the north of the Seine River, the Pays de Caux plateaus are incised by a few larger valleys with perennial streams and numerous smaller dry valleys. The karstic chalk plateaus of the Haute-Normandy region form part of the western edge of the Paris Basin and dip gently (<10°) to the east.

Structural features are characterized by a series of lineaments oriented N45W. The aquifer matrix is almost exclusively chalk, rich in chert and dating from the mid-Cretaceous. Jurassic and lower Cretaceous calcareous marls and clays outcrop along anticlines. Thick surficial formations cover the karstified chalk and are composed of a red clayey, silty sand, corresponding to the residue of chalk alteration, tertiary sands, and reworked ancient loess (Laignel 1997). The thickness of this overall chalk-covering formation ranges from 5 to 10 m.

Hydrogeology

Groundwater moves from the uplands of the chalk aquifer towards the lowlands via rapid drainage through karst conduits and via slower drainage through the fracture porosity of chalk. The chalk aquifer constitutes a quite important reservoir owing to its high matrix porosity—up to 42%, as described by Masson (1978) in Maqsoud (1996). However, the matrix permeability is quite low, with a hydraulic conductivity around 10^{-6} m s^{-1} (Laignel 2003) due to poor pore connectivity (0.5% of effective porosity according to Calba (1980)). Discharge occurs both through springs (mean discharge of around 10–100 L s^{-1}) at the base of the chalk cliffs (with several tens of major springs along the lower Seine Valley) and through the porous alluvial aquifer of the valley which sustains the Seine River baseflow.

The study site, the Bebec-Hannetot karst system within the Norville karst system, is located on the north side of

 DOI 10.1007/s10040-005-0010-3

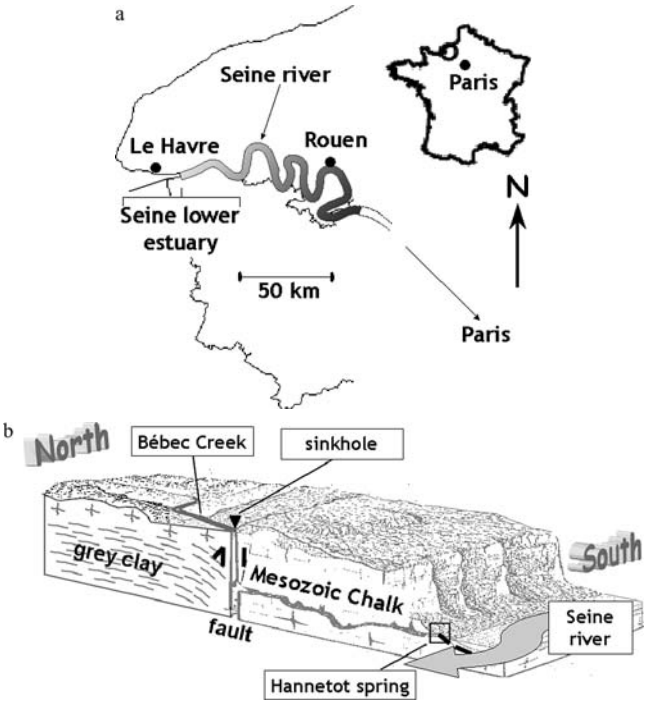

Fig. 1 **a** Location of the study site in the lower Seine Valley, France; **b** geomorphologic three-dimensional diagram of the Bébec-Hannetot karstic system

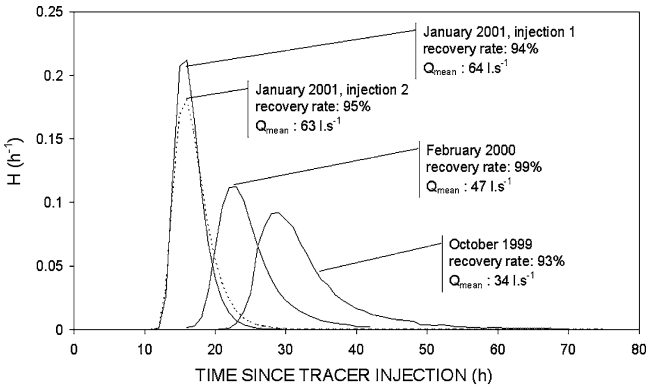

Fig. 2 Residence time distribution for each tracer test (peak areas = 1). Residence time distributions ordinates are $H(t)$=tracer flux/recovered mass

the Seine River, ≈40 km east of the Seine estuary (Fig. 1a). This system is typical of the karst of the lower Seine Valley, the spring being located at the interface between the Seine alluvium and the karstic chalk, as is depicted schematically in Fig. 1b. The Norville system has been widely studied and is relatively well understood (Massei 2001; Massei et al. 2002). The boundaries of the system are well constrained, partially due to its relatively small size (≈10 km^2); it consists of one main major sinkhole on the plateau where Bébec Creek disappears underground only to resurge at Hannetot Spring located at the base of the plateau at a place called "Le Hannetot" in the town of Norville. Hannetot Spring is of vauclusian type; it is an overflow spring (Field 2002) and a barrier spring (Field 2002), resulting from the fine semi-permeable alluvial deposits covering the chalk aquifer in the Seine Valley. The alluvium partially blocks groundwater flow, causing a portion of the groundwater to discharge at the springs, but the main portion flows down gradient under the fine alluvium, the only outlet being the bed of the Seine River. During major rain events, soil erosion causes high turbidity in the water of Bébec Creek, which is then introduced into the sinkhole. Thanks to several quantitative tracer tests during the past 30 years and dissolved/particle transport analyses (Massei 2001; Massei et al. 2003), the Hannetot Spring is clearly identified as being the main outlet of waters swallowed into the sinkhole.

For this reason, the site of Norville, and more precisely, the Bébec-Hannetot karst system, has been the subject of several tracing experiments, the aim of which is a better understanding of the hydrological behaviour of similar systems in the region.

Field and laboratory instrumentation

The tracer used was Na-fluorescein and commonly known as uranine (CI Acid Yellow 73). Field equipment consisted of ISCO 6700 automatic samplers that were installed at both the Bébec sinkhole and Hannetot Spring. Spring discharge was measured using a 15-min time step with an ISCO 4150 Doppler flowmeter. Water samples were analysed using a Turner Designs Model 10-AU filter fluorometer.

Tracer experiments

Description of the four tracer tests

Four tracer tests were conducted during periods of no rainfall, so as to avoid a strong variability of flow rate at both Bébec Creek and Hannetot Spring during the experiment. The four tracer-test breakthrough curves are shown in Fig. 2 as residence time distributions, with the ordinates H(t) representing the instantaneous measured tracer flux/total recovered mass. This type of representation is commonly used for comparing tracer tests, since the area under each curve equals 1 regardless of the tracer recovery rate. The mean transit times (time since tracer input) have a range of 16 to 29 h (Fig. 2). First-order observations of the residence time distributions show that curves exhibit more spread with decreasing spring discharge (Q) and that modal times increase linearly with decreasing spring discharge. The tracer recovery rate is always very high, regardless the spring discharge.

Two tracer injections were implemented in January 2001 using different tracer masses. On 16 January 2001 (injection 1 in Fig. 2), 0.5 kg of uranine were injected into Bébec sinkhole at 4.00 p.m. and was followed by 1 kg of uranine at 8.30 p.m. (injection 2 in Fig. 2). The second injection was basically designed to occur later coinciding with a rain event. The aim was to automatically inject the tracer along with turbidity so as to compare particle and solute transport. However, due to a likely failure of the injection device programming, the tracer was accidentally injected only 4.5 h after the first injection, which explains the quite unusual design of this January 2001 tracer test. The global residence time distribution was then bimodal and the corresponding

 DOI 10.1007/s10040-005-0010-3

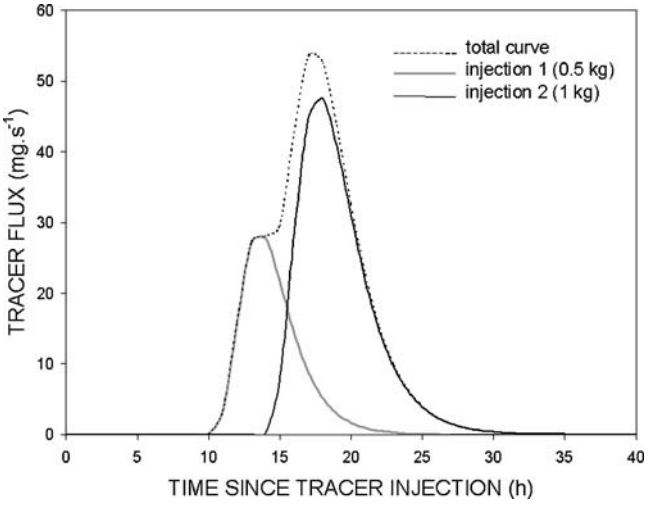

Fig. 3 Bimodal breakthrough curve for the January 2001 tracer experiment, represented as tracer flux. The curve is decomposed in 2 signals, each corresponding to one impulse injection of tracer (0.5 and 1 kg respectively), showing a linear behaviour of the system with respect to mass transport

fluxes were decomposed by means of the PeakFit 4.0 software (SPSS Inc.) resulting in a global curve consisting of a linear combination of two curves, each corresponding to an impulse injection (Fig. 3).

Determination of the karst-conduit parameters by the Qtracer2 program

Tracing tests do not provide information about the whole karst system, but rather only provide information on the part usually referred to as the 'tracing system' (Molinari 1976). In the study example, the tracing system is composed of a conduit connecting the input to the output and the surrounding porous and fissured rock.

The Qtracer2 program (Field 2002) was first used to estimate the volume of the tracing system, the mean apparent velocity (*U*m), the Reynolds number (Nr), the shear velocity ($U_{SHEAR)}$ and the thickness of the viscous sublayer against the wall of the conduit. According to Field (1997) and Field and Nash (1997), the Qtracer2 program provides a reasonable assessment of the flow dynamics of many karstic hydrosystems. The hydrodynamic parameters estimated from the four tracer tests are summarized in Table 1. Although the values listed in Table 1 only represent a rough approximation of the reality, their comparison can be used to evaluate the effect of flow-rate on the hydraulic functioning of the system. The volume of the tracing system was around 3,000 m^3. As flow rate increased, flow-channel volume tended to increase, turbulence tended to increase, and the thickness of the viscous sublayer tended to decrease. The increasing channel volume, which actually represents the volume of the tracing system, suggests that a greater part of the system is flooded, which can be explained by a higher water table within the chalk aquifer (piezometric heads of 29, 33, 37 m in October 1999, February 2000 and January 2001, respectively).

Assessment of the hydrodispersive parameters of the karst system: mathematical background

Both the Chatwin method (Qtracer2: Field (2002)) and the linear graphical method (Wang 1987) have been used for tracer residence time distributions interpretation and hydrodispersive parameter determination. Each of these two methods are based on the analytical solution for an infinite medium of the one-dimensional advective-dispersive equation that can be written as (Wang 1987):

$$C(t) = \frac{W}{t^{0.5}} \exp\left[\frac{P}{4t_m}\frac{(t_m - t)^2}{t}\right] \quad (1)$$

with

$$W = \frac{mx}{Q_m\sqrt{4\pi D_L}} \quad (2)$$

where $C(t)$ is the tracer concentration at time t, m the quantity of tracer injected, x the distance from the injection point, Q_m the flow-rate, D_L the longitudinal dispersion coefficient, P the Péclet number defined as $P = xU_m/D_L$ (where U_m is the tracer mean velocity), and t_m the mean transit time is defined as $t_m{=}x/U_m$.

Hydrodispersive parameters by the Qtracer2 program

The Chatwin method consists of the calculation of the dispersion coefficient based on the following equation (Chatwin 1971):

$$\sqrt{t_i \ln\left(\frac{C_p\sqrt{t_p}}{C_i\sqrt{t_i}}\right)} = \frac{x}{2\sqrt{D_L}} - \frac{U_m t_i}{2\sqrt{D_L}} \quad (3)$$

Table 1 Karst-conduit parameters estimates by the Qtracer2 program

Tracing	Q_m (l s^{-1})	U_m (m h^{-1})	*Nr*	Flow-channel volume estimate (m^3)	U_{SHEAR} (m h^{-1})	Viscous sublayer (mm)
Oct-1999	34	107.0	28 096	3,011	55.9	1.5
Feb-2000	47	139.8	38 777	3,360	70.2	1.2
Jan-2001 (1)	64	227.0	64 084	3,479	112.7	0.7
Jan-2001 (2)	63	173.2	55 797	3,480	78.8	1.1

Q_m is the mean spring discharge, U_m the mean apparent flow velocity, *Nr* the Reynolds number (type of the flow regime), U_{SHEAR} is the shear velocity (i.e., against the wall of the conduit)

 DOI 10.1007/s10040-005-0010-3

where C_p is the peak concentration and t_p is the modal time. The statement of this method and its applications are described in Chatwin (1971), Field (1997) and Field (2002). It was developed by linearizing the one-dimensional analytical solution of the advection-dispersion equation. The method consists of taking into account the rising limb of the residence time distribution only (from step i to the peak of the residence time distribution), which prevents an overestimation of dispersion due to the asymmetrical shapes created by tailing effects.

Hydrodispersive parameters determined via the linear graphical method

The linear graphical method (MGL) was used in the same way for the interpretation of the four tracer tests. The MGL accounts for one or more (<10) layers, which allows for the interpretation of multiple-layer flow and transport. This method allows the experimental points to be subjectively accounted for during the fitting procedure so that just the rising limb of the experimental curve can be fitted or the entire residence time distribution can be fitted, depending on the quality of data. Its principle is described in Wang (1987). It is also developed by linearizing the analytical solution to the one-dimensional advection-dispersion equation after having derived it. Taking the logarithm of Eq. (1) yields:

$$\ln (C\, t^{0.5}) = \ln\, W - \frac{P(t_m - t)^2}{4 t_m\, t} \tag{4}$$

and taking the derivative of Eq. (4) with respect to t yields:

$$\frac{d\, \ln (C\, t^{0.5})}{dt} = a\, T + b \tag{5}$$

with $T=1/t^2$, $a= Pt_m/4$, and $b=-P/4t_m$. Equation (5) is solved using a numerical procedure (finite difference discretization) for the experimental pairs of the values (C,t).

Breakthrough tailing

The results of the breakthrough curves interpretation obtained from the Chatwin method (Qtracer2) are shown in Table 2. The Chatwin method suggests increasing Péclet numbers ($P=x/\alpha$) as a function of increasing flow rate and thus decreasing dispersivity values (α), assuming a constant length x of the system.

Table 2 Hydrodispersive parameters of the Norville karstic system calculated according to each tracer test with the Qtracer2 program

Tracing	Q_m (l s^{-1})	t_m (h)	P	α (m)	Recovery rate (%)
Oct-99	34	30.8	167.6	19.7	88.2
Feb-00	47	23.6	174.3	18.9	94.4
Jan-01 (1)	64	14.5	259.4	12.7	94.6
Jan-01 (2)	63	19.1	256.3	12.9	95.4

Hydrodispersive parameters of the Norville karstic system calculated according to each tracer test with Qtracer2

Q_m=mean spring discharge, t_m=mean transit time, P= Péclet number, α- dispersivity

The four tracer tests were interpreted using the one and two-layer modes of the linear graphical method (MGL), the latter assuming two different layers with different transport and dispersive parameters (flow velocity and dispersivity). The multiple-layer mode allows the operator to account for distinct parts (or, for example, layers in the case of multi-layer aquifer) that may display different transport properties. In this case they, the two-layer mode was used to test the possibility of modelling breakthrough tailing according to the hypothesis that flow can be separated into two parts (turbulent core and pseudo-laminar flow due to shear stresses against walls, or to the presence of sediment within the conduit). The results obtained are as follows:

I. Basing the fit on the rising limb of the residence time distributions, as was done using Qtracer2, necessarily implies a second curve to be added to the first (which is fitted to the rising limb) to obtain a good fit of the entire residence time distribution as a consequence of tailing effects. The corresponding results are summarized in Table 3 and shown in Fig. 4a–d. In Table 3, the hydrodispersive parameters of the Norville karstic system are calculated according to each tracer test via the linear graphical method. The January 2001 residence time distributions (injections 1 and 2), which did not show significant tailing effect, have been interpreted using both the one- and two-layer transport model. Figure 4 shows (a) the October 1999 tracer test: a strong tailing effect is clearly visible; (b) the February 2000 tracer test: the tailing effect is still fairly well expressed; (c) the January 2001 tracer test, injection 1: the tailing effect is poorly expressed; (d) the January 2001 tracer test, injection 2: the breakthrough curve shows similar characteristics as for injection 1.
II. The residence time distributions for January 2001 (Fig. 4c, d; highest flow-rates of 64 and 63 l s^{-1} respectively) were also interpreted in the one-layer mode which suggested good visual fits (Fig. 5a, b). The corresponding Péclet numbers were lower than those obtained from the Qtracer2 program and from the two-layer mode of MGL for curve 1 (e.g., fitted on the rising limb). Actually, the results of the January 2001 tracer tests give Péclet numbers of about 100, whereas they are about 250 when calculated with the Qtracer2 program (see Table 2) and 188–240 for the MGL in the two-layer mode (Table 3).

The calculation of the karst-conduit and hydrodynamic parameters of the system with Qtracer2 showed that drainage could be separated into two parts. Field and Pinsky (2000) have suggested that mobile-immobile flow zones are responsible for the evident dual-flow phenomena, but this study demonstrates that the dual-flow phenomena can also occur as a turbulent core drainage and a surrounding pseudo-laminar drainage. A plot of the Reynolds number Nr and the viscous sublayer thickness against mean spring discharge Q_m (Fig. 6) illustrates this separation of drainage where the viscous sublayer thickness decreases as

 DOI 10.1007/s10040-005-0010-3

Table 3 Hydrodispersive parameters via the linear graphical method (1 or 2-layer flow model)

	Tracing	tm_1 (h)	tm_2 (h)	Um_1 (m h^{-1})	Um_2 (m h^{-1})	P_1	P_2	α_1 (m)	α_2 (m)	Percentage of layer 2 to total area (%)
2-layer	Oct-99	29.1	38.5	113.4	85.7	153.4	92.9	21.5	35.5	26
	Feb-00	22.0	29.1	Err 503	113.4	163	130.6	20.2	25.3	21
	Jan-01 (1)	15.9	19.1	207.5	172.8	240.2	136.6	13.7	24.2	19
	Jan-01 (2)	16.1	20.1	205.0	164.2	188.1	140.7	17.5	23.5	22
1-layer	Jan-01 (1)		16.4		201.2	101.5			32.5	–
	Jan-01 (2)		16.7		197.6	93.3			35.4	–

tm_1, Um_1, P_1, α_1 are the mean transit time, mean apparent tracer velocity, Péclet number and longitudinal dispersivity of each separated curve (or "layer") of Fig. 4

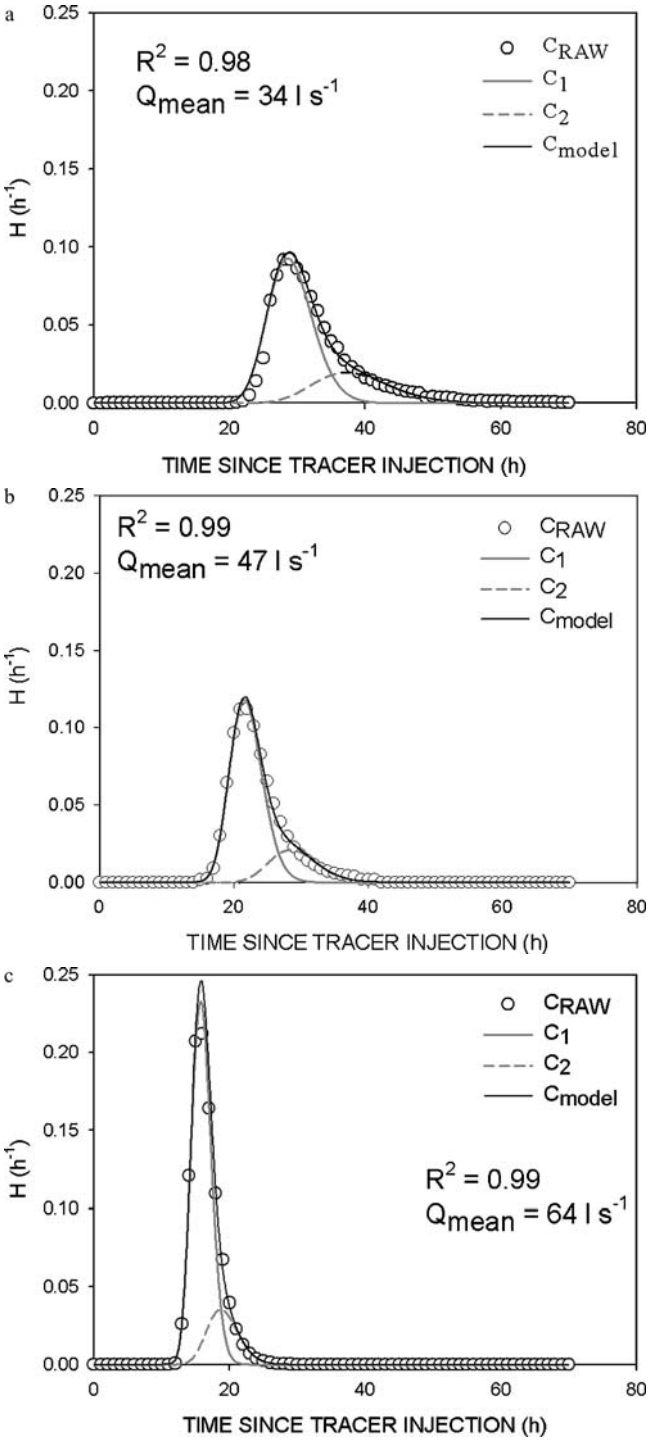

Fig. 4 Tracer breakthrough curves expressed as residence time distribution (ordinates $H(t)$ in h^{-1}) interpreted with the linear graphical method (Wang 1987) in the 2-layer mode. C_{RAW}, C_{model}, C_1 and C_2 are the measured, modelled, first and second separated curves, respectively, and R^2 represents the goodness of fit. Tracer test results are shown for **a**) October 1999 **b**) February 2000 **c**) January 2001, injection 1, and **d**) January 2001, injection 2

DOI 10.1007/s10040-005-0010-3

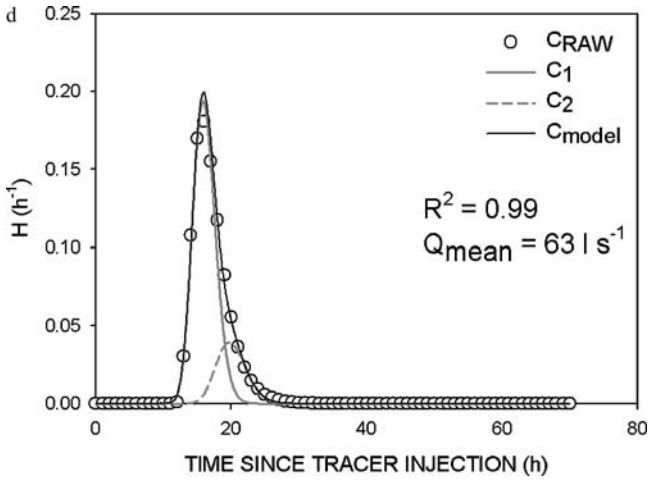

Fig. 4. Continued

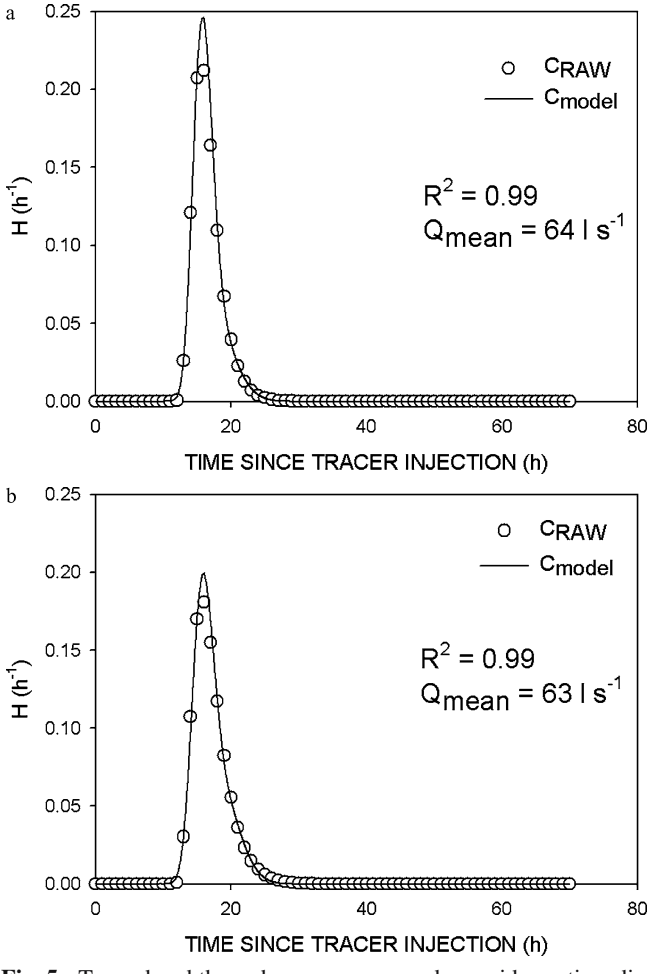

Fig. 5 Tracer breakthrough curves expressed as residence time distributions (ordinates $H(t)$ in h^{-1}) interpreted with the linear graphical method (Wang 1987) in the 1-layer mode for **a**) injection 1 of January 2001, and **b**) injection 2 of January 2001. C_{RAW}, C_{model}, C_1 and C_2 are the measured, modelled, first and second separated curves, respectively, and R^2 represents the goodness of fit

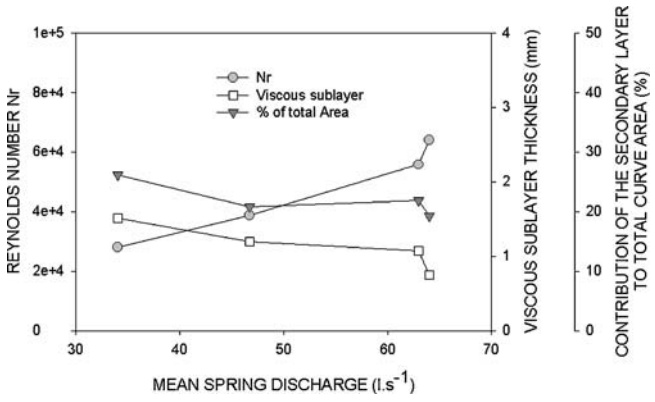

Fig. 6 Reynolds number, viscous sublayer thickness and area contribution of the second curve (2-layer mode) to the total residence time distribution area, plotted against the mean spring discharge

flow-rate increases. Such a duality of flow is in agreement with the interpretations of tracer tests by the linear graphical method, which shows that the residence time distributions can be separated into two curves. Tables 1 and 3 show that the values of velocity U_{m2} associated with the second layer of the two-layer flow model are closer to U_{SHEAR} than the first layer. In addition, the percentage of contribution by the second curve to the total area of the residence time distribution decreases as flow-rate increases, which is also the case for the viscous sublayer (Fig. 6). As flow-rate increases, the part of drainage associated with the viscous sublayer decreases and so does the corresponding solute transport component (i.e., the contribution of the second curve to the total area of the residence time distribution).

However, as stated above, for the highest flow-rates, the transport parameters calculated using the one-layer MGL exhibit significant differences with respect to those calculated with Qtracer2, although a good model fit to the residence time distributions was obtained (Fig. 5a, b). This was not the case when experimental data were interpreted using the two-layer model, where the dispersive parameters obtained were the same as those calculated with Qtracer2 (Tables 2 and 3). This result would suggest that the most reliable interpretation may be obtained by using the rising limb of the residence time distribution only, although a good fit may be obtained with the total curve. As a consequence, a comparison of the results obtained with the one-layer mode with those of the two-layer mode appears to be an imperative requirement whenever applying the MGL.

Hydrodynamic and geomorphologic implications

Geomorphologically, the Norville karst system corresponds to a well-established karst-conduit system with a main conduit capable of assuming all the flow. A similar penetrable system located a few hundred meters away from Hannetot Spring is likely to provide a good representation of the Norville system: the penetrable system displays a single main conduit with a cross-section of around 1 m^2 with

DOI 10.1007/s10040-005-0010-3

no drastic morphological variations. The residence time distributions were expected to be interpreted with a two-layer model for higher flow-rate. Indeed, the dual-porosity (or dual-permeability) phenomena could have resulted in strong tailing effects. Such phenomena would have been due to increasing hydraulic head (and water table elevation) in the aquifer involving flow within weakly drained zones (fissures) or immobile fluid regions that could progressively release solute into the mobile flow region. Moreover, the increase in conduit volume with increasing flow-rate supports such a hypothesis. However, the observed tailing effects correspond with low flow-rates. A dual-permeability interpretation, as proposed by Maloszewski et al. (2002), based on increasing hydraulic head, would not match the observations. Karst-conduit parameters calculated using Qtracer2 clearly indicate that drainage occurs in a dual form. A turbulent flow component constitutes the drainage core with a pseudo-laminar flow (within the viscous sublayer) developed along the conduit walls due to friction forces. Not taking into consideration the effect of the viscous sublayer will cause the dispersion to be underestimated (Chatwin, 1971). The interpretation of data from this study matches these observations, since the increase in the viscous sublayer thickness is linked to an increase of the tailing effects on residence time distributions. So, in the same way that flow can be considered as dual, the transport of dissolved tracer can be separated into two parts with each being related to one type of flow. Turbulent core flow implies strong advective transport with high Péclet numbers ($160<P<250$), whereas that portion of the tracer in the viscous sublayer ($90<P<140$) would be transported more slowly. Hence, the dispersivity values calculated for the turbulent component range from 13.7 to 21.5 m for the first curve of the two-layer mode, which approximates those calculated using the Qtracer2 program (12.7–19.7 m). The dispersivity values calculated for the second component of flow (e.g., the viscous sublayer) are higher, ranging from 23.4 to 35.5 m.

However, a 1 mm-thick boundary layer is not likely to produce such a secondary curve; obviously, the values of the viscous sublayer thickness computed by Qtracer2 are not to be taken as they are. The calculated values allow identification of a flow partitioning phenomenon which could involve many parameters such as wall roughness, conduit morphology, sinuosity, sediment content, etc. This partitioning effect would produce a partitioning of mass transport that can be modelled as a secondary transport component corresponding to a second smaller curve resulting from the separation of the total breakthrough curve. The values of U_{SHEAR} calculated by Qtracer2 support the hypothesis: calculating the transit times corresponding to these values gives 59, 47, 29 and 42 h for Oct. 1999, Feb. 2000, Jan. 2001 injection 1 and Jan. 2001 injection 2, respectively. These U_{SHEAR}-based transit times correspond quite well to the longer times measured on the breakthrough curves of Fig. 2, which would show that the lower velocities are actually related to a purely hydrodynamic effect.

Conclusion

This study addresses the issue of the quantitative interpretation of tracing experiments in karstic media. The inverse approach, which consists of determining the structural and functional properties of a system as well as the transport processes from the results of tracer tests, should be applied with caution when attempting to quantify dispersion properties. The two methods discussed here can, in certain instances, produce very different results. When applied to the entire residence time distribution, the MGL yields dispersivity values twice those obtained by Qtracer2 for high flow rates despite the very good fit of the model to the experimental data. Similar results are obtained when just the rising limb of the residence time distribution is fitted in the same way as was done with Qtracer2. The MGL, because of its flexibility, enhances the quantitative analysis of tracer residence time distributions. Nevertheless, a systematic comparison of the results obtained for a fit of the rising limb and of the entire curve appears necessary. From a technical standpoint, fitting the rising limb of a residence time distribution (or of any breakthrough curve) appears more reliable than fitting the entire curve, although a good match is obtained at first sight.

For the Norville karstic hydrosystem and similar ones (relatively simple residence time distributions), the methods of interpretation (one- or two-layer mode) should be compared. Use of the MGL coupled to the Qtracer2 program showed that:

1. These two methods, based on the analytical solution of the one-dimensional advection-dispersion equation, are very reliable, as previous studies have shown (Field 2002; Field 1997; Lacroix et al. 2000; Massei et al. 2002; Wang 1987), although they may sometimes lead to slightly different results.
2. There is an improvement in the understanding of the functioning of the Norville karstic hydrosystem, considering both the qualitative (typical karstic functioning where flow is well organized through main conduits, with a weak influence of rock fracturing with respect to hydrodynamics and transport) and quantitative aspects (evidence of a duality of flow and transport regardless of flow-rate, and quantification of the dispersion parameters for each type of flow).

The coupled utilization of the MGL and the Qtracer2 program provides good results for the analysis of solute transport properties and the structural characterization of karstic hydrosystems. It also provides a possible model for fitting the tailing effect of the breakthrough curves by considering the existence of the two main transport/hydraulic behaviour components (rapid turbulent component, slower component due to friction forces) and quantifying their respective parts. It obviously demonstrates that, despite the existence of a high-porosity medium around the conduit, the tracing tests and breakthrough tailing can successfully be interpreted as resulting in a flow in a single conduit only, without any exchange with the matrix around it (especially

 DOI 10.1007/s10040-005-0010-3

considering the extremely low matrix hydraulic conductivity of chalk), contrary to the dual-porosity models generally used. These latter models could lead to misinterpretations of both the structure and the functioning of the hydrosystems, although a good agreement was obtained between the modelled and fitted data. Hence, the physical processes highlighted here, obviously without resolving the global problem of breakthrough tailing, have to be accounted for when studying the transport processes, especially when contaminant transport is of concern, since breakthrough tailings may not only be explained by dual-porosity phenomena.

Acknowledgements The authors would like to gratefully thank the Seine-Normandie Water Agency (AESN) for financial support. We would also like to thank the reviewers for their very significant help in improving this paper.

References

Bracq P, Hanich L, Delay F, Crampon N (1992) Mise en évidence par traçage d'une relation rapide, entre la surface et les eaux souterraines, liée à des phénomènes de dissolution dans la craie du Boulonnais (Nord de la France) [Evidence of a rapid connection between surface and ground waters related to chalk dissolution phenomena in the Boulonnais region (northern France)]. Bull Soc Géol Fr 163(2):195–203

Calba F (1980) Hydrogéologie du karst crayeux du pays de Caux (France). Etude de deux bassins. [Hydrogeology of the chalky karst of Pays de Caux (France)], Université Pierre et Marie Curie, Paris, p 189

Chatwin PC (1971) On the interpretation of some longitudinal dispersion experiments. J Fluid Mech 48(4):689–702

Cornaton F, Perrochet P (2002) Analytical 1D dual-porosity equivalent solutions to 3D discrete single-continuum models. Application to karstic spring hydrograph modelling. J Hydrol 262(1–4):165–176

Desmarais K, Rojstaczer S (2002) Inferring source waters from measurements of carbonate spring response to storms. J Hydrol 260(1–4):118–134

Dzikowski M, Delay F, Sauty JP, Crampon N, de Marsily G (1995) Convolution a debit variable a partir des reponses de tracages artificiels; application a un systeme karstique (Causse de Gramat, Lot, France) [Convolution in time-dependent system from artificial tracer test responses; application on a karst system (Causse de Gramat, Lot, France)]. J Hydrol 164(1–4):305–324

Emblanch C, Zuppi GM, Mudry J, Blavoux B, Batiot C (2003) Carbon 13 of TDIC to quantify the role of the unsaturated zone: the example of the Vaucluse karst systems (southeastern France). J Hydrol 279(1–4):262–274

Fairchild IJ, Borsato A, Tooth AF, Frisia S, Hawkesworth CJ, Huang Y, McDermott F, Spiro B (2000) Controls on trace element (Sr-Mg) compositions of carbonate cave waters: implications for speleothem climatic records. Chem Geol 166(3/4):255–269

Field M (2002) The Qtracer2 program for tracer breakthrough curve analysis for tracer tests in karstic aquifers and other hydrologic systems. EPA/600/R-02/001, United States Environmental Protection Agency, Washington, DC

Field MS (1997) Risk assessment methodology for karst aquifers: (2) solute-transport modeling. Environ Monitor Assess 47(1):23–37

Field MS, Nash SG (1997) Risk assessment methodology for karst aquifers: (1) Estimating karst conduit-flow parameters. Environ Monitor Assess 47(1):1–21

Field MS, Pinsky PF (2000) A two-region nonequilibrium model for solute transport in solution conduits in karstic aquifers. J Contam Hydrol 44(3/4):329–351

Grasso DA, Jeannin P-Y, Zwahlen F (2003) A deterministic approach to the coupled analysis of karst springs' hydrographs and chemographs. J Hydrol 271(1–4):65–76

Hauns M, Jeannin P-Y, Atteia O (2001) Dispersion, retardation and scale effect in tracer breakthrough curves in karst conduits. J Hydrol 241(3-4):177–193

Herczeg AL, Leaney FWJ, Stadler MF, Allan GL, Fifield LK (1997) Chemical and isotopic indicators of point-source recharge to a karst aquifer, South Australia. J Hydrol 192(1–4):271–299

Katz BG, Bullen TD (1996) The combined use of 87Sr/86Sr and carbon and water isotopes to study the hydrochemical interaction between groundwater and lakewater in mantled karst. Geochim Cosmochim Acta 60(24):5075–5087

Katz BG, Catches JS, Bullen TD, Michel RL (1998) Changes in the isotopic and chemical composition of ground water resulting from a recharge pulse from a sinking stream. J Hydrol 211(1–4):178–207

Lacroix M, Beaudeau P, Wang H, Massei N, Dupont J (2000) Turbidité en Pays de Caux : un karst concret [Turbidity in the Pays de Caux (Haute-Normandie, France): a problematic karst]. Bull Inf Assoc Géol Bass Paris 37(1):37–40

Laignel B (2003) Caractérisation et dynamique érosive de systèmes géomorphologiques continentaux sur substrat crayeux [Characterization and dynamics of erosion in geomorphologic systems on chalk substratum], University of Rouen, Mont-Saint-Aignan, France, p 138

Laignel B (1997) Les altérites à silex de l'Ouest du bassin de Paris: caractérisation lithologique, genèse et utilisation potentielle comme granulats [Alterites-with-flints of the Western Paris Basin: lithologic characterization, genesis and potential use as aggregate]. PhD Thesis, University of Rouen, Mont-Saint-Aignan, 224 p

Lee ES, Krothe NC (2001) A four-component mixing model for water in a karst terrain in south-central Indiana, USA. Using solute concentration and stable isotopes as tracers. Chem Geol 179(1–4):129–143

Lee ES, Krothe NC (2003) Delineating the karstic flow system in the upper Lost River drainage basin, south central Indiana: using sulphate and [delta]34SSO4 as tracers. Appl Geochem 18(1):145–153

Mahler B, Lynch F (1999) Muddy waters: temporal variation in sediment discharging from a karst spring. J Hydrol 214(1–4):165–178

Maloszewski P, Stichler W, Zuber A, Rank D (2002) Identifying the flow systems in a karstic-fissured-porous aquifer, the Schneealpe, Austria, by modelling of environmental 18O and 3H isotopes. J Hydrol 256(1/2):48–59

Maqsoud A (1996) Approche hydrologique et hydrochimique du caractère karstique éventuel d'hydrosystèmes souterrains de la craie du bassin de Paris [A hydrological and hydrochemical approach for characterization of karst features in the chalk of the Paris Basin]. PhD Thesis, University of Lille I (USTL), Lille, France, pp 323

Massei N (2001) Transport de particules dans l'aquifère crayeux karstique et à l'interface Craie/alluvions [Transport of particles in the Chalk karst aquifer and at the Chalk/alluvium interface]. PhD Thesis, University of Rouen, Mont-Saint-Aignan, France, pp 195

Massei N, Lacroix M, Wang H, Mahler B, Dupont J (2002) Transport of suspended solids from a karstic to an alluvial aquifer: the role of the karst/alluvium interface. J Hydrol 260(1–4):88–101

Massei N, Wang HQ, Dupont JP, Rodet J, Laignel B (2003) Assessment of direct transfer and resuspension of particles during turbid floods at a karstic spring. J Hydrol 275(1/2):109–121

Molinari J (1976) Perspectives offertes par l'utilisation rationnelle des traceurs naturels et artificiels en hydrologie karstique. Commentaires de nombreux exemples récents de multitraçages [On the use of natural and artificial tracers in karst hydrology: some comments of recent examples of multitracing experiments]. Ann Sci Univ Besançon Géol 25:275–306

Pinault J, Plagnes V, Aquilina L, Bakalowicz M (2001) Inverse modeling of the hydrological and the hydrochemical behavior of hydrosystems: characterization of karst system functioning. Water Resour Res 37(8):2191–2204

Quinlan JF, Ewers RO (1985) Ground water flow in limestone terranes: strategy rationale and procedure for reliable, efficient monitoring of ground water quality in karst areas. 5th National symposium and exposition on aquifer restoration and ground water monitoring, 1985, Columbus, Ohio, National Water Well Association, Westerville, OH

Uliana MM, Sharp J, John M (2001) Tracing regional flow paths to major springs in Trans-Pecos, Texas using geochemical data and geochemical models. Chem Geol 179(1–4):53–72

Wang H (1987) Modélisation des transferts de masse en milieu saturé à double porosité; application aux écoulements convergents en craie fissurée semi-confinée et multicouche [Modelling mass transfer in dual-porosity saturated media; application to convergent flow in multilayer semi-confined and fissured chalk]. PhD Thesis, University of Paris XI, Paris

Wang HQ, Crampon N (1995) Method for interpreting tracers experiments in radial flow using modified analytical solutions. J Hydrol 165:11–31

Wang HQ, Crampon N, Huberson S, Garnier JM (1987) A linear graphical method for determining hydrodispersive characteristics in tracer experiments with instantaneous injection. J Hydrol 95(143–154)

White WB (2002) Karst hydrology: recent developments and open questions. Eng Geol 65(2/3):85–105

 DOI 10.1007/s10040-005-0010-3